Journal Homepage: https://dergipark.org.tr/tr/pub/isibted

Isı Bilimi ve Tekniği Dergisi

Archive: https://tibtd.org.tr/dergi

Experimental Investigation of Effects of Nanorefrigerants on Vapor Compression Refrigeration System Using R1234yf Instead of R134a

Kemal BİLEN [1, *], Kayhan DAĞIDIR [2], Erol ARCAKLIOĞLU [1]

[1] *Ankara Yıldırım Beyazıt Üniversitesi, Mühendislik ve Doğa Bilimleri Fakültesi, Makine Mühendisliği Bölümü, Keçiören, 06010, Ankara, Türkiye*
[2] *Tarsus Üniversitesi, Mühendislik Fakültesi, Makine Mühendisliği Bölümü, Tarsus, 33400, Mersin, Türkiye*

A R T I C L E   I N F O

2024, vol. 44, no.2, pp. 280-293
©2024 TIBTD Online.
doi: 10.47480/isibted.1563896

Research Article
Received: 17 July 2023
Accepted: 07 September 2024

* *Corresponding Author*
e-mail: kemal.bilen@aybu.edu.tr

Keywords:
R134a and R1234yf
Al_2O_3
Graphene
CNT
VCRS

ORCID Numbers in author order:
0000-0003-1775-7977
0000-0003-0499-1764
0000-0001-8073-5207

A B S T R A C T

In this study, the refrigerant R1234yf was subjected to experimental investigation in conjunction with a variety of nanoparticles as a potential alternative to R134a in a vapor compression refrigeration system. Initially, the performance of pure R1234yf was evaluated in the absence of modifications to the VCRS, employing energy and exergy analyses. The results demonstrated that R1234yf resulted in a 9% increase in compressor power input, an 8% reduction in cooling capacity, and a 17% decrease in EER in comparison to R134a. Furthermore, the second law efficiency exhibited a decline of 8%. In order to address these declines, Al_2O_3, graphene, and CNT nanoparticles were introduced to the VCRS with R1234yf via compressor oil at varying mass fractions. The greatest improvement in system performance was observed with the addition of 0.250% graphene by mass. This resulted in a 24% and 14% enhancement in cooling capacity and an increase in EER by 32% and 13%, respectively, when compared to pure R1234yf and R134a. The second law efficiency exhibited a slight improvement with the addition of graphene.

R134a Yerine R1234yf Kullanılan Buhar Sıkıştırmalı Soğutma Sisteminde Nanosoğutucu Akışkanların Etkilerinin Deneysel Olarak İncelenmesi

M A K A L E   B İ L G İ S İ

Anahtar Kelimeler:
R134a ve R1234yf
Al_2O_3
Grafen
CNT
BSSS

Ö Z E T

Bu çalışmada, soğutucu akışkan R1234yf, buhar sıkıştırmalı bir soğutma sisteminde (BSSS'nde) R134a'ya potansiyel bir alternatif olarak çeşitli nanopartiküllerle birlikte deneysel olarak incelemeye tabi tutulmuştur. Başlangıçta, saf R1234yf'nin performansı, enerji ve ekserji analizleri kullanılarak BSSS'de değişiklik yapılmadan değerlendirilmiştir. Sonuçlar, R1234yf'nin R134a'ya kıyasla kompresör güç girişinde %9 artışa, soğutma kapasitesinde %8 azalmaya ve EER'de %17 düşüşe neden olduğunu göstermiştir. Ayrıca, ikinci yasa verimliliği %8'lik bir düşüş sergilemiştir. Bu düşüşleri gidermek için, Al_2O_3, grafen ve CNT nanopartikülleri, değişen kütlesel karışım oranlarında kompresör yağı aracılığıyla R1234yf içeren BSSS'ye eklenmiştir. Sistem performansındaki en iyi iyileşme kütlece %0,250 grafen ilavesinde gözlenmiştir. Kütlece %0,250 grafen ilave edilen sistem, saf R1234yf ve R134a'lı durumlarla karşılaştırıldığında soğutma kapasitesinde sırasıyla %24 ve %14'lük ve EER'de %32 ve %13'lük bir artış göstermiştir. İkinci yasa verimliliğinde ise grafen ilavesi ile küçük miktarda bir iyileşme gözlenmiştir.

NOMENCLATURE

CFC	Clorofluorocarbon
EER	Energy Efficiency Ratio
EEV	Electronic Expansion Valve
Ex	Exergy (kJ)
η	Efficiency
GWP	Global Warming Potential
h	Specific enthalpy (kJ/kg)
HCFC	Hydrocloroflorocarbon
HCFCs	Hydrocloroflorocarbons
HFC	Hydroflorocarbon
HFCs	Hydroflorocarbons
$\dot{m}$	Mass (kg/s)
ODP	Ozone Depletion Potential
P	Pressure (Pa)
POE	Polyolester
$\dot{Q}$	Heat transfer rate (kW)
R	Magnitude of any calculated dependent variables
S	Specific entropy [kJ/(kg·K)]
T	Temperature (K or °C)
u	Uncertainty
UNEP	United Nations Environment Programme
VCRC	Vapor Compression Refrigeration Cycle
VCRCs	Vapor Compression Refrigeration Cycles
VCRS	Vapor Compression Refrigeration System
VCRSs	Vapor Compression Refrigeration Systems
$\dot{W}$	Work (kW)
x	Independent variable
Subscripts	
0	Medium
c	Condensation process
e	Evaporation process
in	Inlet
isen	Isentropic
out	Outlet
R	Refrigerant
s	Constant entropy process
VCRS	Experimental setup
w	Water

INTRODUCTION

Under the guidance of the United Nations (UN), numerous countries have made decisions at different times within the negotiations of climate change, impacting the choice of refrigerants utilized as the working fluid in Vapor Compression Refrigeration Systems (VCRSs). Accordingly, the use of Chlorofluorocarbons (CFCs) was restricted due to the high Ozone Depletion Potential (ODP) with the Montreal Protocol signed in 1987 (UNEP, 1987). Later, use of the Hydrochlorofluorocarbons (HCFCs) and Hydrofluorocarbons (HFCs) was also restricted due to the high Global Warming Potential (GWP) with the Kyoto Protocol signed in 1997 (1997, GCRP). Recently, a reduction schedule of usage of HFCs was prepared to prevent harmful effects of refrigerants on the environment based on GWP value of HFCs in heat pump and air conditioning systems. Accordingly, commercial refrigerators involving HFC with a GWP value of bigger than 150 have been banned as of January 1, 2029 (UNEP, 2016). The primary objective of these protocols is to eliminate the use of refrigerants that are environmentally harmful in terms of ODP and GWP. A summary of impacts of decisions made in various climate change negotiations on refrigerants are shown in Figure 1 (Mota-Babiloni and Makhnatch, 2021; Yang et al., 2021).

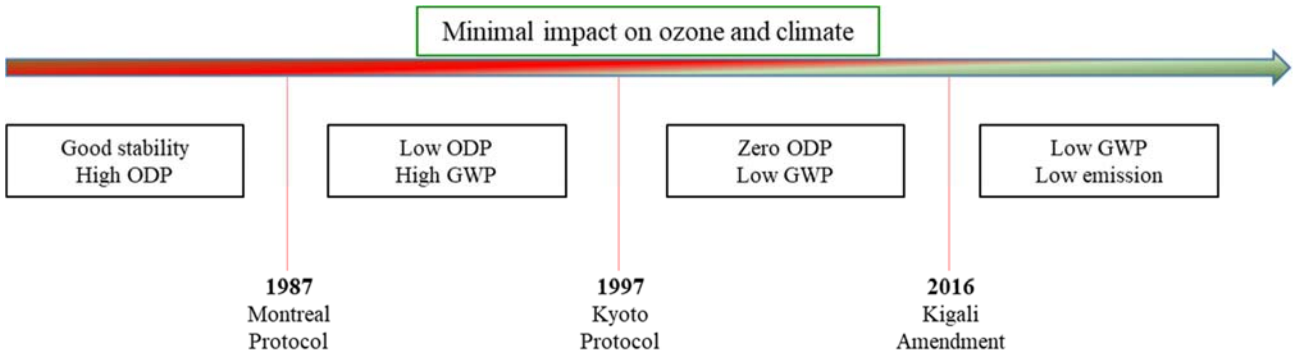

Figure 1. The effects of decisions within the various climate change negotiations on refrigerants.

In the fifth Assessment Report (AR5) by the Intergovernmental Panel on Climate Change (IPCC), R134a, widely favored in refrigeration, air conditioning, and heat pump applications, is noted with a 100-year GWP value of 1 300 (IPCC, 2013). The GWP of R134a is well above the specified limit. Therefore, in the last decade, various alternative refrigerants have been tried instead of R134a (Bilen et al., 2024; Dağıdır and Bilen, 2024). Lately, Hydrofluroolefins (HFOs) have been used as alternative refrigerants in refrigeration applications (Bilen et al., 2023). Recommended as an alternative to R134a, R1234yf is a HFO with a GWP of less than 1 (Arora et al., 2018; Yadav et al., 2022; Li and Tang, 2022). The first studies on R1234yf were related to the replacement of R134a in mechanical VCRSs (Navarro-Esbri et al., 2013). However, it was observed that research involving various system modifications began after it was found that using R1234yf in place of R134a in VCRSs without any modifications led to a decline in performance. (Moles et al., 2014; Li et al., 2014). It has been suggested that various modifications in the system compensate for the drops in system performance (Al-Sayyab et al., 2022; Mishra and Sarkar, 2016). One of the most common modification proposals was to add an internal heat exchanger to the system. Although the use of the internal heat exchanger provided some improvements in system performance, it was not at the desired level. The use of the ejector was another proposed method to compensate for the performance drops in the system. It is possible to state that the usage of the ejector gives better results compared to the usage of internal heat exchangers (Moles et al. 2014). Therefore, studies that require modification to the system, which started with the usage of both an internal heat exchanger and ejector, have become increasingly common. Newly, hybrid studies have been commonly conducted to enhance system performance by implementing multiple modifications simultaneously in VCRSs (Malwe et al., 2022; Khatoon and Karimi, 2023; Erdinc, 2023). However, all these suggested methods require modification in the system and modifying VCRSs may be cause a change in almost all system equipment. It is a more rational approach to turn to methods that do not require modification in the system. Thus, addition of nanoparticles to the refrigerant used in the system can be tried to enhance performance of the VCRSs. It is known that the usage of nanoparticles influences the refrigerants thermal and physical properties such as specific heat capacity, viscosity, density, and thermal conductivity (Sanukrishna et al., 2018; Bhattad et al., 2018; Bilen et al., 2023). Therefore, it is considered that the use of nanoparticles can be accepted as a good alternative method to improve refrigerant thermophysical properties in VCRSs. Refrigerants in VCRSs with nanoparticles are called nanorefrigerants. The term nanorefrigerant refers to the mixture of nanoparticles and refrigerant in VCRSs. However, nanoparticles and refrigerants do not mix easily. It is known that the lubricant of a compressor meets the refrigerant under operating conditions in VCRS. Therefore, the lubricant of the compressor is generally used to mix the nanoparticles with the refrigerant. The working fluid of the systems in which the interactions between the refrigerant and the nanoparticles are provided indirectly is called nanorefrigerant. Soliman et al. (2019) experimentally studied the addition of nanoparticles to the VCRS. It was used as nanoparticles of Al_2O_3 and working fluid of R134a. Results showed that the energy consumption of the system decreased by 10% and actual Coefficient of Performance (COP) increased by 19.5% with the addition of nanoparticles to the system compared to the base system. Salem (2020) experimentally examined the performance of a VCRS using nanoparticles of Carbon Nanotube (CNT) and working fluid of R134a. Results showed that the COP value enhanced up to 37.3% with the addition of nanoparticles to the system compared to the base system. Nair et al. (2020) conducted an experimental study to investigate the effects of adding Al_2O_3 nanoparticles at mass fractions ranging from 0.1% to 0.5% to the VCRS using R134a refrigerant. The study highlighted that the COP of the system increased by 6.5% with the addition of Al_2O_3 nanoparticles. Choi et al. (2021) conducted an experimental investigation into the effects of adding CNT nanoparticles to the VCRS utilizing R134a refrigerant. The study indicated that the COP increased with the increasing volume fraction of the nanoparticles. Subhedar et al. (2022) experimentally examined energy efficiency of the VCRS with the use of nanorefrigerant including Al_2O_3 nanoparticles and R134a refrigerant. The results indicated that the COP increased by up to 85%, while the compressor power input decreased by up to 27% with the addition of 0.075% volume of Al_2O_3 to the system, compared to the baseline system. Akkaya et al. (2023) experimentally investigated the lubrication properties of carbon composites, including Carbon Black (CB), sepiolite (SP), reduced Graphene Oxide (rGO), and CNT in the VCRS. According to the result of the study, usage of nanoparticles SP-rGO provided the best enhancement in COP. In recent years, nanorefrigerants continue to be used in VCRSs with different refrigerants and nanoparticles (Sharif et al., 2022; Ismail et al., 2023; Ogbonnaya et al., 2023).

Nowadays, energy efficiency is becoming more important day by day. However, the performance decrease in alternative refrigerant applications is remarkable. Since the usage of refrigeration, air conditioning, and heat pump systems containing fluorinated greenhouse gases is restricted, the systems currently used must obey the conditions specified in the regulations. However, modification of these VCRSs is both costly and very laborious. It can take a very long time to develop all this system equipment for a new working fluid. In such circumstances, the most rational approach is to investigate methods for effectively utilizing alternative refrigerants without requiring modifications to existing systems. The system performance decreases due to the usage of R1234yf instead of R134a at the same conditions without any modification in the system. Therefore, in this study, R1234yf, R1234yf+Al_2O_3, R1234yf+graphene, and R1234yf+CNTs have been used as alternative working fluid to R134a in VCRSs. It is predicted that the performance drops due to the use of alternative refrigerant R1234yf instead of R134a in the same system without any modification can be compensated with the use of nanorefrigerants. It is considered that the use of nanorefrigerants examined in this study in alternative refrigerant applications will contribute to the literature.

MATERIAL AND METHODS

Test facility

Experimental setup comprises circuits for refrigeration (cooling), condenser and evaporator with water and water including ethylene glycol (EG), respectively. Pivotal equipment of the Vapor Compression Refrigeration Cycle (VCRC) is situated within the circuit of refrigeration, encompassing four primary operations. These operations are delineated as given a) compression, executed by a compressor of reciprocating; b) condensation, transpiring in a plate type heat exchanger with water-cooled; c) expansion, regulated by an Electronic Expansion Valve (EEV); and d) evaporation, transpiring in a plate heat exchanger with water-heated. The EG water mixture (60% water and 40% EG by volume) serves as cooling medium. The evaporation and condensation transpire within dedicated lines, comprising the evaporator EG water mixture line and the condenser water line, respectively. It employs circulation pumps to propel the EG water mixture and water within the evaporator and condenser lines in the closed flow circuits. Heat transfer (cooling) occurs between the EG water mixture and refrigerant in the evaporator, whereas heat transfer (heating) transpires between the refrigerant and water in the condenser. A heat recovery system and a chiller uphold constant temperatures within the EG water mixture and water tanks. Detailed insights into the refrigeration and auxiliary circuits, including a schematic depiction (Figure 2a) and various photographs of the system (Figure 2b), are provided in Figure 2. Furthermore, Table 1 elucidates the components of the system.

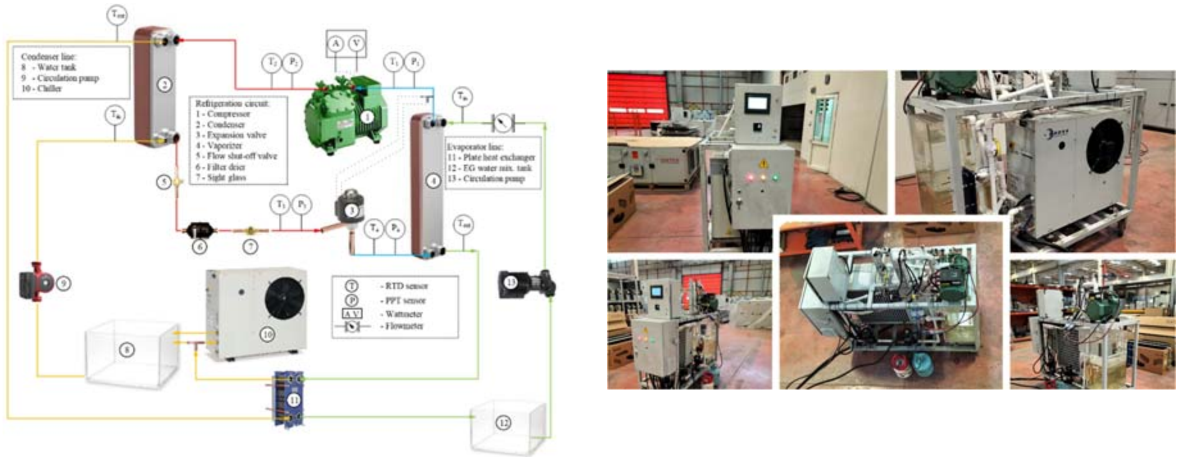

(a) (b)

Figure 2. a) Schematic representation and b) some photos of the test installation.

Table 1. Experimental setup equipment.

Equipment	Specification
1) Compressor	Semi-hermetic BITZER compressor of reciprocating, 4CES-6Y-40S model.
2) Condenser	Plate ALFA LAVAL heat exchanger, AC-30EQ-20H-F model.
3) Throttling device	DANFOSS EEV, model of ETS 6.
4) Evaporator	Plate ALFA LAVAL heat exchanger, AC-70X-20M-F model.
5) Shut-off valve	DANFOSS shut-off valve, GBC model.
6) Filter-drier	DANFOSS filter-dryer, DML model.
7) Sight glass	DANFOSS sight-glass, SGP model.
8) Condenser line tank	64 L capacity.
9) Circulation pump	GRUNDFOS pump for water, UPS2 25-80 model.
10) Chiller	RHOSS chiller, model of THAEY 105.
11) Heat exchanger	Plate ALFA LAVAL heat exchanger, model of T2-BFG.
12) Evaporator line tank	48 L capacity.
13) Circulation pump	GRUNDFOS pump for EG water mixture, TP 25/2 A-O-A-BQQE-AX1 model.

Specific measurement points and strategically positioned measurement devices were carefully selected to perform a comprehensive thermodynamic analysis of the test facility. Temperature and pressure measuring were carried out at these identified points to execute the refrigeration circuit analysis. The Resistance Temperature Detectors (RTDs) were utilized as the temperature measuring device. Also, the Piezoresistive Pressure Transmitters (PPTs) were used as the pressure measuring device. The RTD sensors were utilized to measure not only the refrigerant temperature, but also the water and water including EG temperature at the entrance and exit of both condenser and evaporator. Additionally, ambient temperature was measured using the thermistor named Negative Temperature Coefficient (NTC). Besides, the digital wattmeter was employed in order to monitor the electrical power consumption of the compressor throughout the experiments. Furthermore, the digital turbine-type flowmeter was utilized to determine the volume flow rate for the evaporator EG water mixture line. It can be stated that the measuring range and uncertainty of these measurement devices are matched with those reported in similar studies in the literature (Singh et al., 2021). For more technical details regarding all measurement devices utilized in the experiments, please refer to Table 2.

Table 2. The measurement devices specifications.

Equipment	Measuring range	Uncertainty
Wattmeter	0 ~ 10 kW	±1%
Flowmeter	5 ~ 60 L/min	±1%
RTD sensor	–70 ~ 200 °C	±0.5 °C
PPT sensor	0 ~ 25 bar	±0.25%
NTC sensor	–20 ~ 60 °C	±0.5 °C

In the described test facility, average superheating of 6 °C is consistently maintained using an EEV, a parameter held constant across all tests. Similarly, the setup is configured to achieve the subcooling of 5 °C at the outlet of condenser for R134a. The data collected during the experimental trials are meticulously recorded and monitored by a Programmable Logic Controller (PLC) of the DELTA model. The data logger with sixteen-inputs is utilized to store the measurement data used in analyses. Electrical power, temperature, and pressure measuring could be easily monitored with the help of 7-inch screen of the Delta throughout the tests. Moreover, a separate small screen was allocated for monitoring the volume flow rate. By this way, it was enabled real-time monitoring of all measuring data in experiments.

Refrigerants (working fluids)

In the research, R1234yf was alternatively employed as a refrigerant to commonly used R134a in VCRSs, involving applications in household air conditioners and refrigerators. Diverse properties of R1234yf and R134a are similar such as critical pressure, critical temperature, and molecular weight. The molecular weight of R134a is 102.03 and the molecular weight of R1234yf is 114.04 g/mol. The critical pressure of R134a is 40.59 bar and the critical pressure of R1234yf is 33.42 bar. The critical temperature of R134a is 101.06 and the critical temperature of R1234yf is 94.70 °C. R1234yf is distinguished from other refrigerants by a notably lower GWP value of ~1, in comparison to R134a's value of 1300. This makes it a more environmentally friendly refrigerant. Furthermore, the atmospheric lifetime of R1234yf is considerably shorter, with a duration of approximately 11 days, in comparison to R134a, which remains in the atmosphere for 13 years. Attributes render R1234yf a compelling alternative to refrigerant R134a. For a detailed comparison of the important properties of the refrigerants, please refer to Table 3. Also, latent heat of condensation and evaporation both R134a and R1234yf are assessable with the help of pressure-enthalpy (*P*-*h*) and temperature-entropy (*T*-*s*) diagrams. These diagrams for both R134a and R1234yf are illustrated in Figure 3. Thus, it could be observed that latent heat of both refrigerants is close to each other under the same conditions.

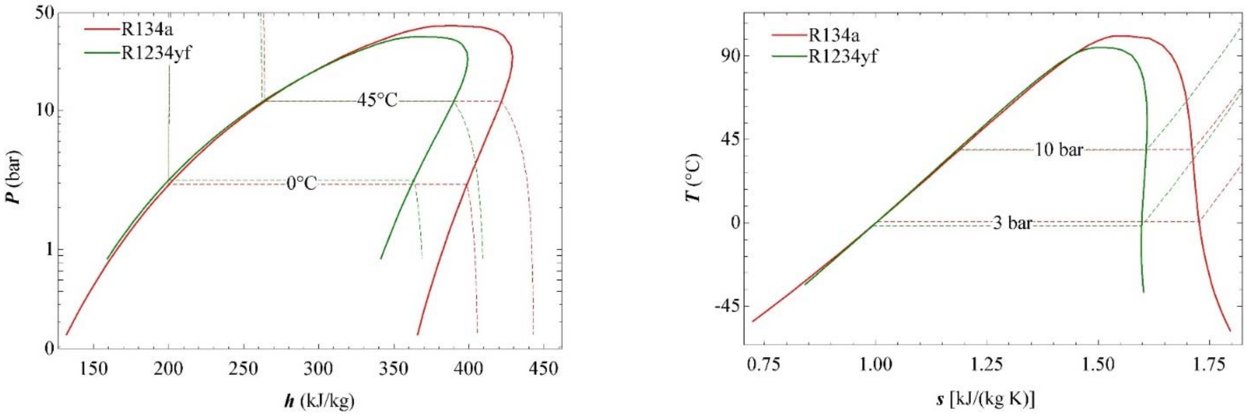

(a) (b)

Figure 3. a) *P*-*h* chart and b) *T*-*s* chart for R134a and R1234yf.

Table 3. Refrigerant properties using this study (Colombo et al., 2020).

Property	**R134a**	**R1234yf**
Chemical name	1,1,1,2 Tetrafluoroethane	2,3,3,3 Tetrafluoropropene
Molecular formula	CH_2FCF_3	CH_2-CF=CF_3
Molecular mass (g/mol)	102.03	114.04
Boiling point (°C) at 1 atm	−25.90	−29.50
Critic temperature (°C)	101.06	94.70
Critic pressure (kPa)	4059	3342.20
GWP_{100} (IPCC, 2013)	1300	<1
ODP	0	0
Atmospheric lifetime	13 years	11 days
Flammability	A1	A2L

Nanorefrigerants preparation

In this study, nanoparticles were introduced into the VCRS through the compressor lubricant, which is Polyolester (POE) oil. The POE oil in the experimental setup is EMKARATE RL 32H matched with both refrigerants. Technical specification of this lubricant is presented in Table 4. It is known that the lubricant of a compressor meets the refrigerant under operating conditions in VCRSs. Therefore, it is important to emphasize that the nanoparticles added to the lubricant also interact with the refrigerant when mixed with the compressor lubricant. Additionally, it can be stated that this contact of the nanoparticles affects the refrigerant. Therefore, the working fluid of such systems is called nanorefrigerant and compressor lubricant including nanoparticle is also called nanolubricant. In scope of this study, R1234yf+Al_2O_3, R1234yf+graphene, and R1234yf+CNTs nanorefrigerants were utilized as the working fluid in the VCRS in place of R134a. Technical specification of nanoparticles used nanorefrigerants is presented in Table 5. Previous studies were also used the same nanoparticles for different purposes (Dağıdır and Bilen, 2023a; Dağıdır and Bilen 2023b). EDS and XRD analyses were performed for each nanoparticle type, and FE-SEM images were given. Thus, it could be stated that characteristics of Al_2O_3 (Prins, 2020), graphene (Dang et al., 2020), and CNTs (He et al., 2020) nanoparticles are compatible with the literature. Given that both graphene and CNTs are carbon-based nanomaterials, while Al_2O_3 is a metal-based nanomaterial, the mass fractions in the lubricant differ from each other. Mass fraction of nanoparticles was determined according to similar studies in literature. Accordingly, minimum mass fraction of Al_2O_3 (Akkaya et al., 2021), graphene and CNTs (Salem, 2020) were selected as 0.250%, 0.125%, and 0.125%, respectively.

Nanoparticles was added step by step to the system using R1234yf starting from the minimum mass fraction. Compressor power input in the system was checked during experiments, thus mass fraction of nanoparticles was raised as compressor power input decrement continued. Experiment for relevant nanorefrigerant type was stopped when the compressor electrical power increased again. Then other nanorefrigerant type was tried similarly. In this way, it was purposed to find the ideal nanoparticles mass fraction.

Table 4. Specifications of the POE oil (Emkarate, 2015).

Feature	**ASTM standard**	**Result**
Kinematic viscosity	D445	32.5 cSt (at 40 °C)
Kinematic viscosity	D445	5.8 cSt (at 100 °C)
Index of viscosity	D2270	121
Density	D1298	0.98 g/mL (at 20 °C)
Flash point	D92	264 °C
Pour point	D97	−55 °C

In this study, a two-step method, commonly employed in similar studies in the literature, was utilized to mix the POE lubricant with nanoparticles (Senthilkumar and Anderson, 2021; Sharif et al., 2022). Mass measuring of the lubricant and nanoparticle is performed with the precision balance with brand named RADWAG PS1000.R2. Initially, nanoparticles and this lubricant were stirred by the mechanical mixer with brand named TOPTION MX-S, later they were mixed by the ultrasonic mixer with brand named TOPTION TU-900E4 again. These mixtures were maintained in an ultrasonic mixer for at least 90 minutes before being charged into the compressor through the lubricating chamber for experiments. This method has been successfully applied in previous studies (Dağıdır and Bilen, 2023a). The devices employed in the two-step method are depicted in Figure 4.

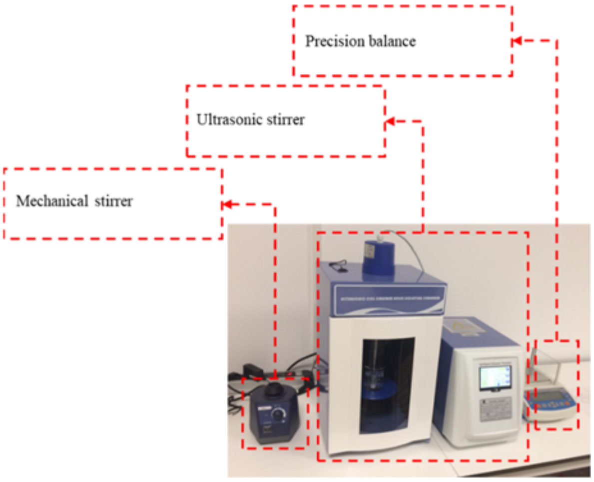

Figure 4. Apparatus utilized in the two-step method.

Nanolubricants stability

During the preparation step, the ultrasonic mixing time is conducted as 90 minutes to provide stability as recommended in the similar research in the literature (Redhwan et al., 2019). Measured zeta potential values for nanolubricants involving Al_2O_3 nanoparticles were compared to a previous study (Zawawi et al., 2022) in literature in Figure 5. According to these values, stability of nanolubricants involving Al_2O_3 nanoparticles is normal at the mass fraction of ω = 1.00% (the highest) and excellent at the mass fraction of ω = 0.25% (the lowest). Stability of all nanolubricants was also considered to be stable since all nanolubricant samples were prepared with the two-step method.

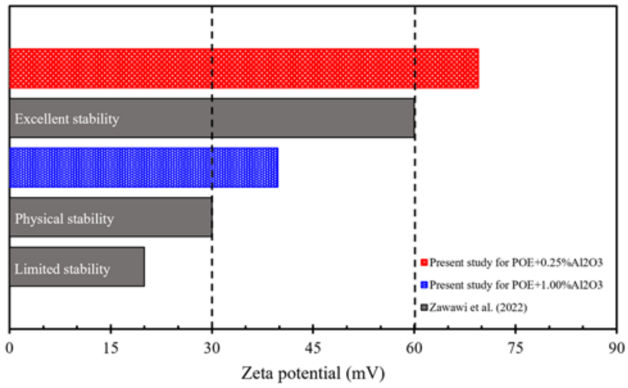

Figure 5. Zeta potential values of nanolubricant samples involving Al_2O_3 nanoparticles.

Table 5. Technical specifications of the nanoparticles (Dağıdır and Bilen, 2023a).

	Al_2O_3	Graphene	CNTs
Properties	Purity: 99.5% Type: Gamma nanoparticles Average particle size: 18 nm Morphology: Nearly spherical Specific surface area:140 m²/g Color: White	Purity: 99.9% Type: Graphene Nanoplatelets Diameter: 18 μm Thickness: 5 nm Specific surface area: 170 m²/g Color: Gray	Purity: 96% Type: Multi-Walled Carbon Nanotube (MWCNT) Inside diameter: 5-10 nm Outside diameter: 8-18 nm Length: 10-30 μm Specific surface area: 220 m²/g Color: Black
FE-SEM images	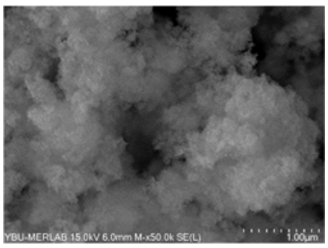	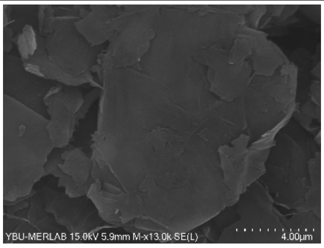	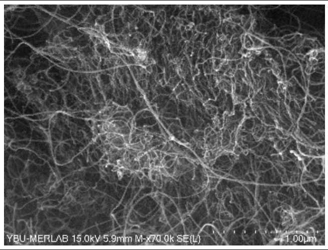
XRD analysis	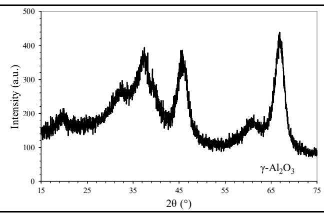	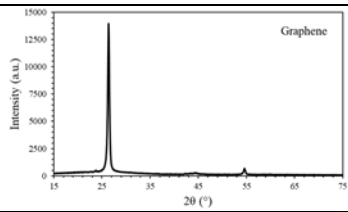	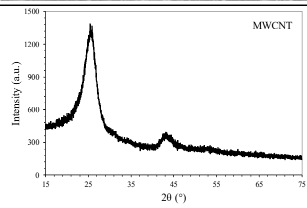

Thermodynamic analyses of the test facility

In this investigation, tests were performed on the VCRS at steady-state steady-flow conditions. Equations were individually obtained for the primary equipment of the system which are the compressor for compression, condenser for condensation, EEV for throttling, and evaporator for evaporation. Thermodynamic assessments of the refrigeration circuit were conducted based on the following assumptions: 1) VCRS equipment operates under steady-state, steady-flow conditions. 2) Heat transfer between the VCRS equipment and the environment is considered negligible. 3) Changes in potential and kinetic energy are disregarded.

Compression in compressor

The requirement compressor energy input per unit time $\dot{W}_{in}$ is specified with the electrical power directly measured using wattmeter throughout experiments. Compression Ratio (CR) in compressor is the ratio of state 2 (discharge) absolute pressure to state 1 (suction) absolute pressure. The isentropic efficiency, η_{isen} is calculated with Eq. (1).

$$\eta_{isen} = \frac{h_{2,s}-h_1}{h_2-h_1} \quad (1)$$

where *h* is specific enthalpy (kJ/kg). Subscripts numbered 1 and 2 refer to state and *s* refers to the isentropic compression process.

The compressor exergy destruction rate, $\dot{Ex}_{dest,comp}$ is calculated with Eq. (2).

$$\dot{Ex}_{dest,comp} = \dot{m}_R T_o (s_2 - s_1) \quad (2)$$

where $\dot{m}$ is the mass flow rate (kg/s), T_0 is ambient temperature, and s is specific entropy [kJ/(kg·K)]. Additionally, subscript *R* refers to the refrigerant.

Condensation in condenser

Heat rejection rate of the condenser, $\dot{Q}_H$, is determined as the sum of cooling capacity and compressor electrical power input. Exergy destruction rate in the condenser, $\dot{Ex}_{dest,cond}$ is calculated by using Eq. (3).

$$\dot{Ex}_{dest,cond} = \dot{m}_R(ex_2 - ex_3) + \dot{m}_w(ex_{w,in} - ex_{w,out}) \quad (3)$$

where subscripts *in* and *out* refer to the *inlet* and *outlet*, respectively, and *ex* is the specific exergy (kJ/kg).

Throttling in EEV

EEV exergy destruction rate, $\dot{Ex}_{dest,exp}$ is calculated with Eq. (4).

$$\dot{Ex}_{dest,exp} = \dot{m}_R(ex_3 - ex_4) \quad (4)$$

where the expansion valve is represented by the subscript *exp*.

Evaporation in evaporator

VCRS's cooling capacity, $\dot{Q}_L$, is determined using Eq. (5).

$$\dot{Q}_L = \dot{m}_{ew}\left(h_{ew,in} - h_{ew,out}\right) \quad (5)$$

where subscript *ew* indicates water including EG in the evaporator.
Evaporator exergy destruction rate, $\dot{Ex}_{dest,evap}$ is calculated with Eq. (6).

$$\dot{Ex}_{dest,evap} = \dot{m}_R(ex_4 - ex_1) + \dot{m}_{ew}(ex_{ew,in} - ex_{ew,out}) \quad (6)$$

where the evaporator is represented by subscript *evap*.

General system performance parameters

The overall performance parameters of the VCRS are represented by the Energy Efficiency Ratio (EER) as energetic performance indicator and second law efficiency as exergetic performance indicator.

EER of the VCRS, EER_{VCRS}, is determined as the heat transfer rate in the evaporator (cooling capacity) per the compressor electrical power input as represented in Eq. (7).

$$EER_{VCRS} = \frac{\dot{Q}_L}{\dot{W}_{in}} \quad (7)$$

VCRS's exergy efficiency, $\eta_{ex,VCRS}$, is determined as in Eq. (8). VCRS's total exergy destruction rate, $\dot{Ex}_{dest,total}$ is the sum of the exergy destruction rate obtained for each equipment (De Paula et al., 2020).

$$\eta_{ex,VCRS} = 1 - \frac{\dot{Ex}_{dest,total}}{\dot{W}_{in}} \quad (8)$$

Additionally, refrigerant mass flow rate, $\dot{m}_R$ is determined with the standard named American Society of Heating, Refrigerating and Air-Conditioning Engineers: Standard 41.1-1986 (Sharif et al., 2022) as represented in Eq. (9).

$$\dot{m}_R = \frac{\dot{Q}_L}{h_1 - h_4} \quad (9)$$

The measured temperature and pressure values are used to determine the thermophysical properties in the thermodynamic analysis of the system. The thermophysical properties were determined using the Engineering Equation Solver (EES) software. In the exergy analysis, the ambient temperature was measured and taken as the dead state temperature (T_0). The standard atmospheric pressure was also taken as the dead state pressure (P_0). Other dead state properties such as enthalpy (h_0) and entropy (s_0) were determined depending on the dead state temperature and pressure.

Operating conditions

The experimental setup utilized in this study was designed to operate with R134a as the working fluid. At the same time, in the test facility of this study, an EEV was utilized. This valve adjusts its opening automatically, responding to the refrigerant pressure and temperature at the outlet of evaporator. Supported by electronic control equipment, the EEV plays a crucial mission in maintaining stability of the VCRS by promptly reacting in order to change in system variables. Throughout the experiments, superheating at the evaporator outlet was maintained at approximately 6 °C thanks to the EEV. Refrigerants were incrementally charged into the VCRS until reaching the target superheating value, at which point the tests were conducted. The EEV also provided a standardized approach to refrigerant charging. Thus, the charge amount of R134a refrigerant was approximately 700 g and the charge amount of R1234yf refrigerant was approximately 780 g. The comparison of results was based on constant evaporation and condensation temperatures. Experiments were conducted at approximately 0 °C and 45 °C temperatures for evaporation and condensation, respectively. Firstly, R134a was tested under these test conditions, then R1234yf was used instead of R134a without any modification in the system and pure refrigerant tests were completed. After this stage, nanoparticles were added by means of compressor oil to the system using R1234yf. Also, the filter-drier in the system was replaced with a new one for each type of nanoparticle. It was observed that the addition of nanoparticles has both positive and negative effects, as in similar studies in the literature (Pawale et al., 2017). Thus, it was understood that there was an upper limit to the mass fraction of nanoparticles added to the system. Mass fractions of 0.75% for Al_2O_3 and 0.250% for graphene and CNTs yielded the most significant improvements in system performance parameters under the operating conditions evaluated in this study.

ERROR ANALYSIS

Error analysis is a crucial aspect of validating experimental examination. In practical terms, various approaches are devised to pinpoint errors in obtained parameters with the help of data gathered from tests. Among the approaches, uncertainty analysis stands out as one of the most employed approaches. Thus, the uncertainty of any magnitude, contingent upon measuring data, is given as shown in Eq. (10).

$$u_R = \pm\left[\left(\frac{\partial R}{\partial x_1}u_{x_1}\right)^2 + \left(\frac{\partial R}{\partial x_2}u_{x_2}\right)^2 + \left(\frac{\partial R}{\partial x_3}u_{x_3}\right)^2 + \cdots + \left(\frac{\partial R}{\partial x_n}u_{x_n}\right)^2\right]^{1/2} \quad (10)$$

where x is independent variable, R is any measured magnitude, u is uncertainty.

The EES software was employed for calculating uncertainties. The uncertainty determined for the EER, indicating the energetic performance of the VCRS, is between 5.74%-6.75%. Likewise, the uncertainty obtained for the exergy efficiency, reflecting the exergetic performance of the VCRS, is between 7.24%-8.10%. It was observed that the obtained uncertainty values were consistent with findings in the literature (Al-Sayyab et al., 2022).

RESULTS AND DISCUSSIONS

In this experimental research, R1234yf, R1234yf+Al_2O_3, R1234yf+graphene, and R1234yf+CNTs were investigated as alternative refrigerants to R134a concerning their thermodynamic properties, without any modifications to the system. Accordingly, the results related to effects of the usage of R1234yf+Al_2O_3, R1234yf+graphene, and R1234yf+CNTs nanorefrigerants in the system were shared. An EEV was employed in the test facility of this study. Throughout the experiments, superheating at the evaporator outlet was maintained at approximately 6 °C thanks to throttling device. Working fluids were charged gradually into the VCRS up to desired value of superheating and experiments were performed at this value. The comparison of the results was based on approximately 0 °C and 45 °C temperatures for evaporation and condensation, respectively.

Validation of the study

Initially, the test results were validated by comparing the actual and ideal pressure-specific enthalpy (*P-h*) and temperature-specific entropy (*T-s*) diagrams of the system using R134a with previous studies found in the literature (Morales-Fuentes, 2021; Al-Sayyab et al., 2022). Moreover, the reciprocating compressor compatible with R134a is certified by a respected organization named Association of European Refrigeration Component Manufacturers (ASERCOM). Thus, validation experiments were carried out in the test installation using R134a at the same conditions. Results of the validation experiments were compared with the results of the ASERCOM data, focusing on *P-h* and *T-s* charts as given in Figure 6a and Figure 6b, respectively. Accordingly, it could be stated that results of these verification tests align well with both the ASERCOM data and ideal cycle data. Subsequently, EER values calculated in the validation study were compared to the ASERCOM results and this comparison is depicted in Figure 6c. It could be concluded that these EER values fall within reasonable limits, consistent with the certified data. Finally, R1234yf was used as the working fluid instead of R134a in this study. The EER value declined when R1234yf was used in place of R134a under the same conditions in the VCRS. This EER decrease was compared to the previous studies (Sanchez et al., 2017; Li et al., 2019; Chen et al., 2020; Alkan et al., 2021) in literature. Results obtained are given in Figure 6d. Consequently, the EER decreases in previous studies in the literature and the EER decrease in this study are at similar levels. Accordingly, it is considered that the experiments are reliable.

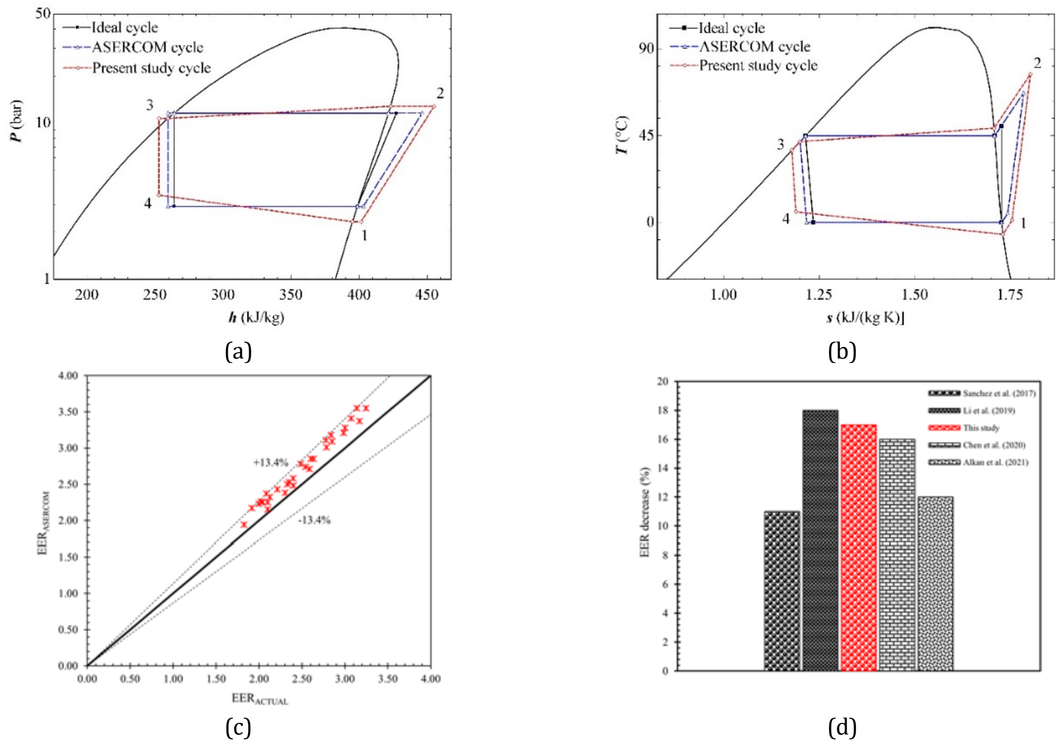

Figure 6 The a) *P-h* diagram and b) *T-s* diagram of ideal, actual, and ASERCOM cycles, c) comparison of actual and ASERCOM systems in view of EER values, d) comparison of this study and previous studies in terms of decrease in EER.

Discussions on the experimental results

In this study, it was predicted that the performance decrease caused by the usage of an alternative refrigerant R1234yf instead of R134a in the VCRS could be compensated by adding nanoparticles to the system without any modifications. The results of the study showed that the nanoparticles added to the VCRS improved the system performance parameters. It was observed that the addition of nanoparticles has both positive and negative effects, as in the similar studies in the literature (Pawale et al., 2017). While the positive effects prevail due to the favorable thermal and tribological properties of the compressor oil and refrigerant up to a certain mass ratio, the negative effects become predominant beyond that ratio due to the instability of the mixture and increased friction (Kaushik et al., 2021). Thus, there is a limit for mass fraction of nanoparticles added to the system. For the operating conditions of this study, these limits are 0.75% for Al_2O_3, and 0.250% for both graphene and CNTs. Since CNTs and graphene are carbon-based nanomaterials, their optimum mass fractions are similar. However, since Al_2O_3 is a metal-based nanomaterial, it has an optimum mass fraction different from graphene and CNTs. The results have shown that the system performance starts to deteriorate in case of exceeding these optimum mass fractions of nanoparticles. Performance parameters of the system containing pure refrigerants and nanorefrigerants are discussed in the following section.

Results about compressor performance parameters

The variation of compressor power input for pure refrigerants and nanorefrigerants is seen in Figure 7. Therefore, it was observed that the increase in compressor power input resulting from the use of R1234yf instead of R134a in the VCRS was nearly offset by the addition of nanoparticles. The variation of the compression ratio for pure refrigerants and nanorefrigerants is shown in Figure 8. Thus, it was seen that the compression ratio increased with the usage of nanorefrigerant in the system. The variation of the compressor isentropic efficiency for pure refrigerants and nanorefrigerants is given in Figure 9. Thus, it was seen an increase in the compressor isentropic efficiency at similar operating conditions with the use of carbon-based nanorefrigerant compared to R134a. Maximum increment in isentropic efficiency was obtained by around 16% at graphene mass fraction of 0.250% compared to R134a. The variation of compressor exergy destruction rate for pure refrigerants and nanorefrigerants is seen in Figure 10. Hence, it was observed a decrease in compressor destruction rate at similar operating conditions with the usage of nanorefrigerant up to 29% at a graphene mass fraction of 0.250% compared to R134a.

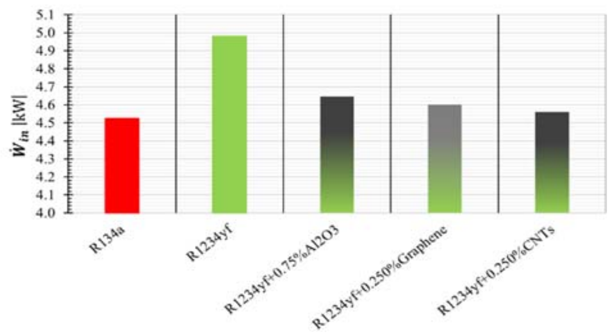

Figure 7. Variation in the compressor power input based on the working fluid.

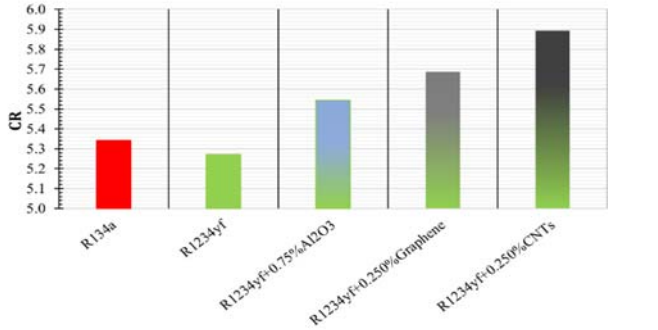

Figure 8. Variation of the compression ratio with the working fluid.

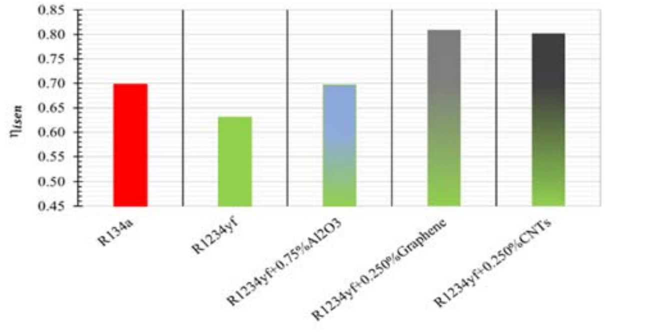

Figure 9. Variation of the compressor isentropic efficiency with the working fluid.

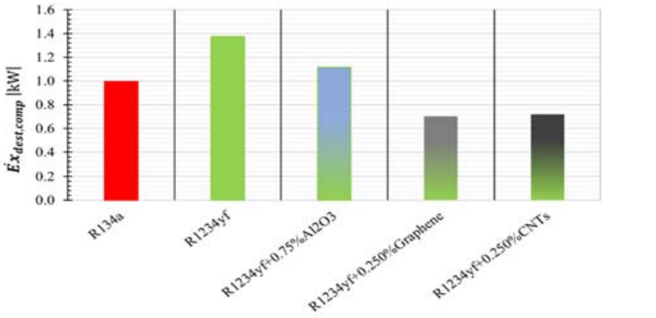

Figure 10. Variation of the compressor exergy destruction rate with the working fluid.

Results about condenser performance parameters

The changing of heat rejection rate for pure refrigerants and nanorefrigerants in the condenser is given in Figure 11. It was seen that the condenser heat rejection rate increased with the usage of nanorefrigerant. This maximum increment rate was approximately 11% at graphene mass fraction of 0.250% compared to R134a. The variation of the condenser exergy destruction rate for pure refrigerants and nanorefrigerant is shown in Figure 12. Accordingly, it was observed that the exergy destruction rate of the condenser increased with the use of nanorefrigerant. This maximum increment rate was nearly 9%.

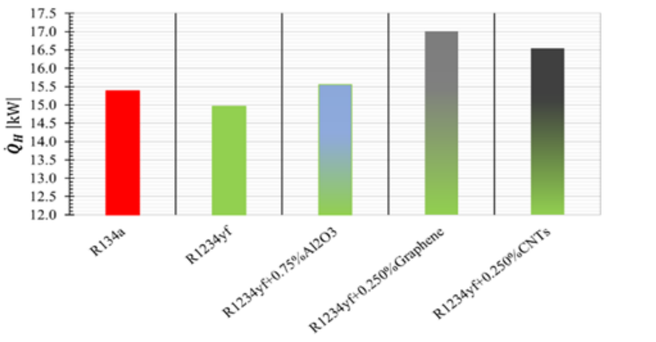

Figure 11. Variation in heat rejection rate within the condenser based on the working fluid.

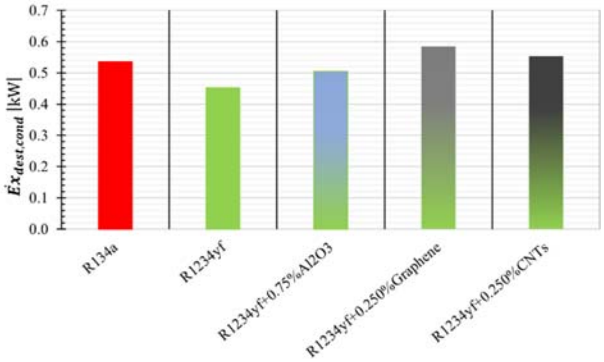

Figure 12. Variation of the condenser exergy destruction rate with the working fluid.

Results about EEV performance parameters

The variation of EEV exergy destruction rate for pure refrigerants and nanorefrigerants is given in Figure 13. It was seen that the EEV exergy destruction rate reduced up to 23% by using nanorefrigerant at the CNTs mass fraction of 0.250%.

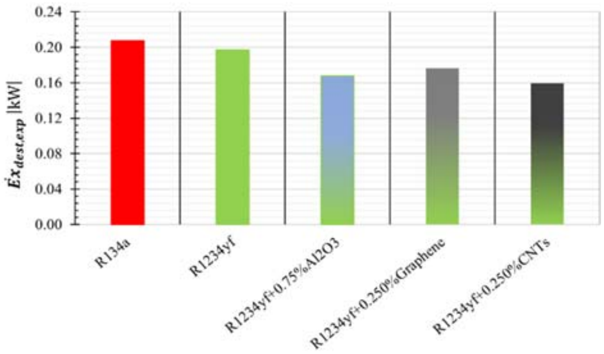

Figure 13. Variation of exergy destruction rate in the EEV with the working fluid.

Results about evaporator performance parameters

The variation of cooling capacity for pure refrigerants and nanorefrigerants is given in Figure 14. Accordingly, the cooling capacity increased up to 14% with the addition of graphene to the system with R1234yf compared to the usage of R134a. The variation of the evaporator exergy destruction rate for pure refrigerants and nanorefrigerant is given in Figure 15. It was noted that the exergy destruction rate in the evaporator increased with the use of nanorefrigerant. The maximum increment in the evaporator exergy destruction rate was by around 68% at the usage of R1234yf+0.250% graphene nanorefrigerant.

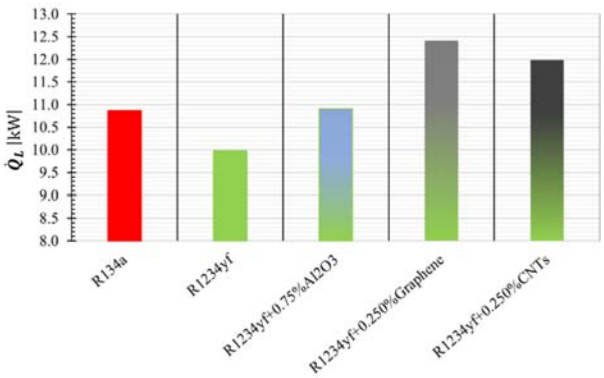

Figure 14. Variation of the cooling capacity in the system with the working fluid.

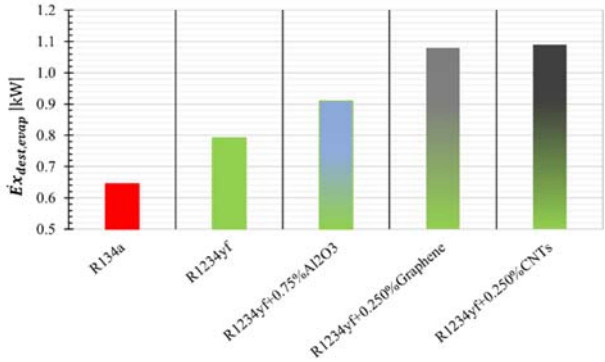

Figure 15. Variation of the evaporator exergy destruction rate with the working fluid.

Results about overall system performance parameters

The usage of carbon-based nanoparticles was better than Al_2O_3 in increasing the system performance. On the other hand, the usage of graphene nanoparticles is better than CNTs in terms of system performance parameters. The EER value of the system increased because of the increase in the cooling capacity. The cooling capacity increased up to 14% with the addition of graphene to the system with R1234yf compared to the usage of R134a. The variation of EER for pure refrigerants and nanorefrigerants is given in Figure 16. Accordingly, it revealed that EER, which was an expression of overall system energetic performance, increased up to 13% with the usage of R1234yf+graphene nanorefrigerants in the system compared to the usage of R134a. Besides, the VCRS's total exergy destruction rate for both pure refrigerants and nanorefrigerants is given in Figure 17. It was observed that total exergy destruction rate slightly increased in respect to the VCRS including R134a. Additionally, the VCRS's exergetic efficiency is shown in Figure 18. It was also seen that there was no significant change in exergy efficiency in all cases. Consequently, it was emphasized that the VCRS with R1234yf containing graphene nanoparticles at the mass fraction of 0.250% had the best system performance among all cases.

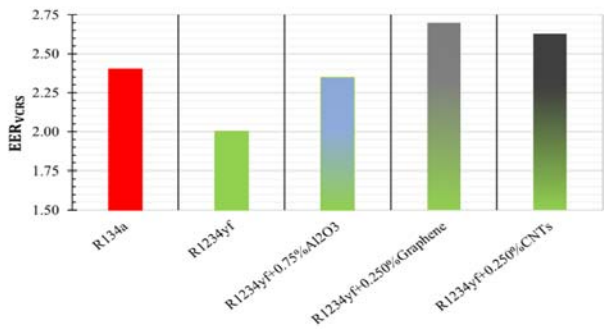

Figure 16. Variation of the EER value of the system with the working fluid.

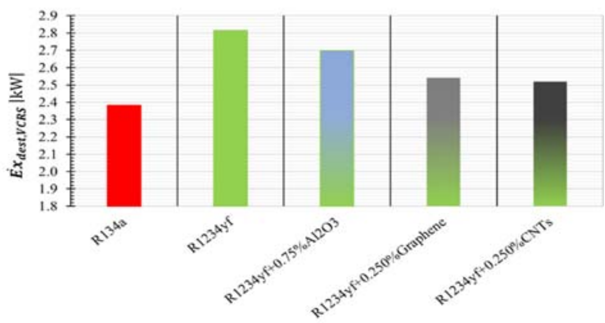

Figure 17. Variation of the total exergy destruction rate of the system with the working fluid.

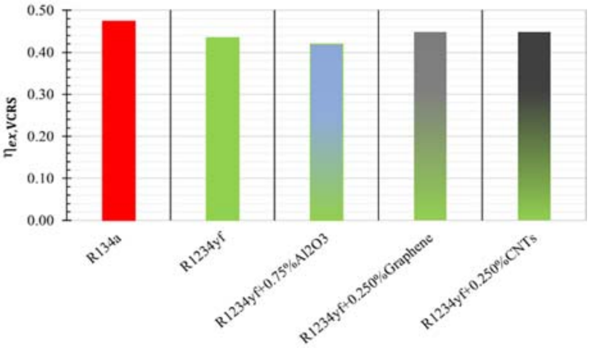

Figure 18. Variation in the second law efficiency of the system as a function of the working fluid.

As a result of this study, it was found that the energetic performance parameter, EER, increased by approximately 13% when using R1234yf with nanoparticles compared to using pure R134a in the VCRS. This increase cannot be directly compared with previous studies in the literature because no study has been identified in the literature testing R1234yf with nanoparticles instead of R134a in the system. Therefore, this study can be indirectly compared to previous studies. For example, previous studies in the literature on the use of R134a with nanoparticles in VCRS are summarized in Table 6. It is considered as an important advantage that this study obtained an increase close to the EER increment obtained by using R134a with nanoparticles compared to the use of pure R134a as shown in Table 6. This is because of the increase in EER obtained in this study by using the alternative refrigerant R1234yf with nanoparticles instead of pure R134a.

Table 6. Energetic performance increases obtained in previous studies in literature.

Reference	Nanoparticle(s)	Finding
Saravanan and Vijayan (2018)	Al_2O_3 and TiO_2	EER raised up to 10.6%
Soliman et al. (2019)	Al_2O_3	EER increased up to 19.5%
Chauhan et al. (2019)	TiO_2	EER increased up to 29.1%
Salem (2020)	CNTs	EER value enhanced up to 37.3%.
Yilmaz (2020)	CuO and Cu/Ag	EER value improved op to 20.88%.
Nair et al. (2020)	Al_2O_3	EER increased up to 6.5%.
Raghavulu and Rasu (2021)	Graphene	EER increased up to 29%.
Afolalu et al. (2021)	ZnO	EER increased up to 15%.
Akkaya et al. (2021)	Al_2O_3	EER increased up to 18.27%.
Arumuganainar et al. (2022)	CeO_2	EER increased up to 7.6%.
Mohamed et al. (2022)	CuO and CeO_2	EER increased up to 25%
Farahani et al. (2022)	SiO_2 and TiO_2	EER increased up to 16.4%.

CONCLUSIONS

In conclusion, the experimental investigation of R1234yf, an environmentally friendly refrigerant, as a working fluid in a VCRS revealed that the system can safely operate with R1234yf without modifications. However, the use of pure R1234yf results in some drops in the system performance parameters compared to R134a. Therefore, Al_2O_3, graphene, and CNTs nanoparticles were introduced into the VCRS using pure R1234yf through the compressor oil to mitigate the performance losses associated with replacing R134a with R1234yf.

The system performance parameters increased with adding nanoparticles up to the optimum mass fraction. Accordingly, in this study, the optimal mass fractions were identified as 0.75% for Al_2O_3, 0.250% for graphene, and 0.250% for CNTs under the same operating conditions. The most significant enhancement in system performance parameters was achieved with the addition of graphene at its optimal mass fraction of 0.250%.

This study examined the use of R1234yf together with nanoparticles as an alternative to R134a in VCRSs experimentally. Similarly, various studies can also be carried out for different alternative refrigerants and nanoparticles in VCRSs. Nevertheless, it is recommended that future studies should compare the service life of system components in VCRSs with and without nanoparticles by means of life cycle testing. In this way, it can be reported whether the lifetime of systems with nanoparticles is shorter than that of systems without nanoparticles. In addition, it can be proposed to investigate whether the addition of nanoparticles has any negative effects on the main and auxiliary elements of the system over time. This is because VCRSs are formed by the combination of many components. Additionally, the typical types of failure to which VCRSs are exposed under operating conditions are known, so that solutions to possible failures can be proposed to final users in advance. In this context, it can be recommended to carry out studies to determine the typical failures of systems with nanoparticles compared to the systems without nanoparticles. Finally, it can be suggested to perform studies on the thermoeconomic analysis of the system with nanorefrigerants. It is believed that reporting the cost of adding nanoparticles to the system under different operating conditions will contribute to developments in this area.

ACKNOWLEDGEMENT

The authors are grateful to TUBITAK (The Scientific and Technological Research Council of TURKEY) for their valuable support to this research with the 1001 project numbered 119M074. Besides, the authors express their gratitude to UNTES Air Conditioning Systems Incorporation for their precious support.

REFERENCES

Afolalu S. A., Ikumapayi O. M., Ogundipe A. T., Yusuf O. O., & Oloyede O. R. (2021). Development of nanolubricant using Aloe Vera plant to enhance the thermal performance of a domestic refrigeration system. *International Journal of Heat and Technology*, 39(6), 1904-1908. https://doi.org/10.18280/ijht.390626

Akkaya M., Menlik T., & Sozen A. (2021). Performance enhancement of a vapor compression cooling system: An application of POE/Al_2O_3. *Journal of Polytechnic-Politeknik Dergisi*, 24(3), 755-761. https://doi.org/10.2339/politeknik.679563

Akkaya M., Sarilmaz A., Balci S., & Ozel F. (2023). Numerical and experimental analysis of refrigerating performance for hybrid nanolubricants with sepiolite additives. *Thermal Science and Engineering Progress*, 37, 101576. https://doi.org/10.1016/j.tsep.2022.101576

Alkan A., Kolip A., & Hosoz M. (2021). Energetic and exergetic performance comparison of an experimental automotive air conditioning system using refrigerants R1234yf and R134a. *Journal of Thermal Engineering*, 7, 1163-1173. https://doi.org/10.18186/thermal.978014

Al-Sayyab A. K. S., Navarro-Esbri J., Barragan-Cervera A., Kim S., & Mota-Babiloni A. (2022). Comprehensive experimental evaluation of R1234yf-based low GWP working fluids for refrigeration and heat pumps. *Energy Conversion and Management*, 258, 115378. https://doi.org/10.1016/j.enconman.2022.115378

Arora P., Seshadri G., & Tyagi A. K. (2018). Fourth-generation refrigerant: HFO 1234yf. *Current Science*, 115(8), 1497-1503. https://doi.org/10.18520/cs/v115/i8/1497-1503

Arumuganainar K., Edwin M., & Raj J. B. (2022). Investigation on the performance improvement of household refrigeration system using R-134a refrigerant blended with ceria nano additives. *Applied Nanoscience*, 12(5), 1753-1761. https://doi.org/10.1007/s13204-022-02365-1

Bhattad A., Sarkar J., & Ghosh P. (2018). Improving the performance of refrigeration systems by using nanofluids: A comprehensive review. *Renewable and Sustainable Energy Reviews*, 82, 3656-3669. https://doi.org/10.1016/j.rser.2017.10.097

Bilen K., Dağidir K., & Arcaklioğlu E. (2022). The effect of nanorefrigerants on performance of the vapor compression refrigeration system: A comprehensive review. *Energy Sources, Part A: Recovery, Utilization, and Environmental Effects*, 44(2), 3178-3204. https://doi.org/10.1080/15567036.2022.2062071

Bilen K., Dağıdır K., Arcaklıoğlu E., & Cansevdi B. (2023). Energy and exergy analysis of R1234yf using instead of R134a in a vapour compression refrigeration system: An experimental study. *International Journal of Exergy*, 42(3), 315-336. https://doi.org/10.1504/IJEX.2023.135517

Bilen K., Işık B., Dağıdır K., & Arcaklıoğlu E. (2024). Thermodynamic analysis of usage of R134a, R1234yf, R450A, R513A, and R515B in the mechanical vapor compression refrigeration system. *Journal of the Faculty of Engineering and Architecture of Gazi University*, 39(1), 161-175. https://doi.org/10.17341/gazimmfd.1203826

Chauhan S. S., Kumar R., & Rajput S. P. S. (2019). Performance investigation of ice plant working with R134a and different concentrations of POE/TiO_2 nanolubricant using experimental method. *Journal of the Brazilian Society of Mechanical Sciences and Engineering*, 41, 163. https://doi.org/10.1007/s40430-019-1657-3

Chen X., Liang K., Li Z., Zhao Y., Xu J., & Jiang H. (2020). Experimental assessment of alternative low global warming potential refrigerants for automotive air conditioners application. *Case Studies in Thermal Engineering*, 22, 100800. https://doi.org/10.1016/j.csite.2020.100800

Choi T. J., Kim D. J., Jang S. P., Park S., & Ko S. (2021). Effect of polyolester oil-based multiwalled carbon-nanotube nanolubricant on the coefficient of performance of refrigeration systems. *Applied Thermal Engineering*, 192, 116941. https://doi.org/10.1016/j.applthermaleng.2021.116941

Colombo L. P. M., Lucchini A., & Molinaroli L. (2020). Experimental analysis of the use of R1234yf and R1234ze(E) as drop-in alternatives of R134a in a water-to-water heat pump. *International Journal of Refrigeration*, 115, 18-27. https://doi.org/10.1016/j.ijrefrig.2020.03.004

Dağıdır K. & Bilen K. (2023a). Experimental investigation of usage of POE lubricants with Al_2O_3, graphene or CNT nanoparticles in a refrigeration compressor. *Beilstein Journal of Nanotechnology*, 14(1), 1041-1058. https://doi.org/10.3762/bjnano.14.86

Dağıdır K. & Bilen K. (2023b). Principles of using nanorefrigerant in a VCRS: An experimental application. *International Journal of Advanced Natural Sciences and Engineering Researches*, 7(3), 38-43. https://as-proceeding.com/index.php/ijanser

Dağıdır K. & Bilen K. (2024). Usage of R513A as an alternative to R134a in a refrigeration system: An experimental investigation based on the Kigali amendment. *International Journal of Thermofluids*, 21, 100582. https://doi.org/10.1016/j.ijft.2024.100582

Dang M. N., Nguyen T. H., Nguyen V., Thu T. V., Le H., Akabori M., Ito N., Nguyen H. Y., Le T. L., & Nguyen T. H. (2020). One-pot synthesis of manganese oxide/graphene composites via a plasma-enhanced electrochemical exfoliation process for supercapacitors. *Nanotechnology*, 31, 345401. https://doi.org/10.1088/1361-6528/ab8fe5

De Paula C. H., Duarte W. M., Rocha T. T. M., De Oliveira R. N., & Maia A. A. T. (2020). Optimal design and environmental, energy and exergy analysis of a vapor compression refrigeration system using R290, R1234yf, and R744 as alternatives to replace R134a. *International Journal of Refrigeration*, 113, 10-20. https://doi.org/10.1016/j.ijrefrig.2020.01.012

Emkarate RL 32H Typical Properties Data Sheet. (2015). The Lubrizol Corporation, USA.

Erdinc M. T. (2023). Performance simulation of expander-compressor boosted subcooling refrigeration system. *International Journal of Refrigeration*, 149, 237-247. https://doi.org/10.1016/j.ijrefrig.2022.12.013

Farahani S. D., Farahani M., & Ghanbari D. (2022). Experimental study of the effect of spiral-star fins and nano-oil-refrigerant mixture on refrigeration cycle characteristics. *Journal of Thermal Analysis and Calorimetry*, 147(11), 6469-6480. https://doi.org/10.1007/s10973-021-10921-0

Global Environmental Change Report GCRP. (1997). A Brief Analysis Kyoto Protocol, vol. IX, p. 24.

He X., Xu X., Bo G., & Yan Y. (2020). Studies on the effects of different multiwalled carbon nanotube functionalization techniques on the properties of bio-based hybrid non-isocyanate polyurethane. *The Royal Society of Chemistry Advances*, 10, 2180-2190. https://doi.org/10.1039/c9ra08695a

Intergovernmental Panel on Climate Change (IPCC), The Physical Science Basis. Contribution of Working Group I to the Fifth Assessment Report of the Intergovernmental Panel on Climate Change. In: Stocker T. F., Qin D., Plattner G.-K., Tignor M. M. B., Allen S. K., Boschung J., Nauels A., Xia Y., Bex V., & Midgley P. M. (2013). Cambridge University Press, Cambridge, United Kingdom, and New York, NY, USA. https://doi.org/10.1017/CBO9781107415324

Ismail M. F., Azmi W. H., Mamat R., Sharma K. V., & Zawawi N. N. M. (2023). Stability assessment of polyvinyl-ether-based TiO_2, SiO_2, and their hybrid nanolubricants. *Lubricants*, 11, 23. https://doi.org/10.3390/lubricants11010023

Kaushik R., Kundan L., & Sharma R. K. (2021). Investigating the performance of nanorefrigerant (R134a+CuO)-based vapor compression cycle: A new scope. *Heat Transfer Research*, 52(13), 33-53. https://doi.org/10.1615/HeatTransRes.2021036516

Khatoon S. & Karimi M. N. (2023). Thermodynamic analysis of two evaporator vapor compression refrigeration system with low GWP refrigerants in automobiles. *International Journal of Air-Conditioning and Refrigeration*, 31(1), 2. https://doi.org/10.1007/s44189-022-00017-1

Li H. & Tang K. (2022). A comprehensive study of drop-in alternative mixtures for R134a in a mobile air-conditioning system. *Applied Thermal Engineering*, 203, 117914. https://doi.org/10.1016/j.applthermaleng.2021.117914

Li H. S., Cao F., Bu X. B., Wang L. B., & Wang X. L. (2014). Performance characteristics of R1234yf ejector-expansion refrigeration cycle. *Applied Energy*, 121, 96-103. https://doi.org/10.1016/j.apenergy.2014.01.079

Li Z. H., Liang K., & Jiang H. Y. (2019). Experimental study of R1234yf as a drop-in replacement for R134a in an oil-free refrigeration system. *Applied Thermal Engineering*, 153, 646-654. https://doi.org/10.1016/j.applthermaleng.2019.03.050

Malwe P. D., Shaikh J., & Gawali B. S. (2022). Exergy assessment of a multistage multi-evaporator vapor compression refrigeration system using eighteen refrigerants. *Energy Reports*, 8, 153-162. https://doi.org/10.1016/j.egyr.2021.11.072.

Mishra S. & Sarkar J. (2016). Performance characteristics of low global warming potential R134a alternative refrigerants in ejector-expansion refrigeration system. *Archives of Thermodynamics*, 37(4), 55-72. https://doi.org/10.1515/aoter-2016-0027.

Mohamed H. A., Camdali U., Biyikoglu A., & Aktas M. (2022). Performance analysis of R134a vapor compression refrigeration system based on CuO/CeO_2 mixture nanorefrigerant. *Journal of the Brazilian Society of Mechanical Sciences and Engineering*, 44(5), 220. https://doi.org/10.1007/s40430-022-03522-x.

Moles F., Navarro-Esbri J., Peris B., Mota-Babiloni A., & Barragan-Cervera A. (2014). Theoretical energy performance evaluation of different single stage vapour compression refrigeration configurations using R1234yf and R1234ze(E) as working fluids. *International Journal of Refrigeration-Revue Internationale Du Froid*, 44, 141-150. https://doi.org/10.1016/j.ijrefrig.2014.04.025.

Morales-Fuentes A., Ramirez-Hernandez H. G., Mendez-Diaz S., Martinez-Martinez S., Sanchez-Cruz F. A., Silva-Romero J. C., and Garcia-Lara H. D. (2021). Experimental study on the operating characteristics of a display refrigerator phasing out R134a to R1234yf. *International Journal of Refrigeration*, 130, 317-329. https://doi.org/10.1016/j.ijrefrig.2021.05.032.

Mota-Babiloni A. & Makhnatch P. (2021). Predictions of European refrigerants place on the market following F-gas regulation restrictions. *International Journal of Refrigeration*, 127, 101-110. https://doi.org/10.1016/j.ijrefrig.2021.03.005.

Nair V., Parekh A. D., & Tailor P. R. (2020). Experimental investigation of a vapour compression refrigeration system using R134a/nano-oil mixture. *International Journal of Refrigeration*, 112, 21-36. https://doi.org/10.1016/j.ijrefrig.2019.12.009.

Navarro-Esbri J., Mendoza-Miranda J. M., Mota-Babiloni A., Barragan-Cervera A., & Belman-Flores J. M. (2013). Experimental analysis of R1234yf as a drop-in replacement for R134a in a vapor compression system. *International Journal of Refrigeration-Revue Internationale Du Froid*, 36(3), 870-880. https://doi.org/10.1016/j.ijrefrig.2012.12.014.

Ogbonnaya M., Ajayi O. O., & Waheed M. A. (2023). Influence of refrigerant type, nanoparticles concentration and size on the performance and exergy efficiency of the vapour compression refrigeration system using Al_2O_3 based nanolubricant. *Journal of Nanofluids*, 12(3), 712-722. https://doi.org/10.1166/jon.2023.1953.

Pawale K. T., Dhumal A. H., & Kerkal G. M. (2017). Performance analysis of VCRS with nano-refrigerant. *International Research Journal of Engineering and Technology*, 4(4), 1031-1037. https://www.irjet.net/archives/V4/i5/IRJET-V4I5201.pdf

Prins R. (2020). Mini-review on the structure of γ-Al_2O_3. *Journal of Catalysis*, 392, 336-346. https://doi.org/10.1016/j.jcat.2020.10.01

Raghavulu K. V. & Rasu N. G. (2021). An experimental study on the improvement of coefficient of performance in vapor compression refrigeration system using graphene lubricant additives. *Energy Sources, Part A: Recovery, Utilization, and Environmental Effects*. https://doi.org/10.1080/15567036.2021.1909186

Redhwan A. A. M., Azmi W. H., Sharif M. Z., Mamat R., Samykano M., & Najafi G. (2019). Performance improvement in mobile air conditioning system using Al_2O_3/PAG nanolubricant. *Journal of Thermal Analysis and Calorimetry*, 135, 1299-1310. https://doi.org/10.1007/s10973-018-7656-2

Salem M. R. (2020). Performance enhancement of a vapor compression refrigeration system using R134a/MWCNT-oil mixture and liquid-suction heat exchanger equipped with

twisted tape turbulator. *International Journal of Refrigeration*, 120, 357-369.
https://doi.org/10.1016/j.ijrefrig.2020.09.009

Sanchez D., Cabello R., Llopis R., Arauzo I., Catalan-Gil J., & Torrella E. (2017). Energy performance evaluation of R1234yf, R1234ze(E), R600a, R290 and R152a as low-GWP R134a alternatives. *International Journal of Refrigeration*, 74, 269-282.
https://doi.org/10.1016/j.ijrefrig.2016.09.020

Sanukrishna S. S., Murukan M., & Jose P. M. (2018). An overview of experimental studies on nanorefrigerants: Recent research, development and applications. *International Journal of Refrigeration*, 88, 552-577.
https://doi.org/10.1016/j.ijrefrig.2018.03.013

Saravanan K. & Vijayan R. (2018). First law and second law analysis of Al_2O_3/TiO_2 nano composite lubricant in domestic refrigerator at different evaporator temperature. *Materials Research Express*, 5, 095015.
https://doi.org/10.1088/2053-1591/aad72d

Sharif M. Z., Azmi W. H., Zawawi N. N. M., & Ghazali M. F. (2022). Comparative air conditioning performance using SiO_2 and Al_2O_3 nanolubricants operating with Hydrofluoroolefin-1234yf refrigerant. *Applied Thermal Engineering*, 205, 118053.
https://doi.org/10.1016/j.applthermaleng.2022.118053

Singh D. K., Kumar S., Kumar S., & Kumar R. (2021). Potential of MWCNT/R134a nanorefrigerant on performance and energy consumption of vapor compression cycle: A domestic application. *Journal of the Brazilian Society of Mechanical Sciences and Engineering*, 43(12), 540.
https://doi.org/10.1007/s40430-021-03240-w

Soliman A. M. A., Rahman A. K. A., & Ookawara S. (2019). Enhancement of vapor compression cycle performance using nanofluids: Experimental results. *Journal of Thermal Analysis and Calorimetry*, 135(2), 1507-1520.
https://doi.org/10.1007/s10973-018-7623-y

Subhedar D. G., Patel J. Z., & Ramani B. M. (2022). Experimental studies on vapour compression refrigeration system using Al_2O_3/mineral oil nano-lubricant. *Australian Journal of Mechanical Engineering*, 20(4), 1136-1141.
https://doi.org/10.1080/14484846.2020.1784558

United Nations Environment Programme (UNEP). (1987). Montreal Protocol on Substances that Deplete the Ozone Layer, Final Act, United Nations, New York.

United Nations Environment Programme (UNEP). (2016) Twenty-eighth Meeting of the Parties to the Montreal Protocol on Substances that Deplete the Ozone Layer, Decision XXVIII/Further Amendment of the Montreal Protocol, 2016:1-9.

Yadav S., Liu J., & Kim S. C. (2022). A comprehensive study on 21st century refrigerants - R290 and R1234yf: A review. *International Journal of Heat and Mass Transfer*, 182, 121947.
https://doi.org/10.1016/j.ijheatmasstransfer.2021.121947

Yang Z., Feng B., Ma H., Zhang L., Duan C., Liu B., Zhang Y., Chen S., & Yang Z. (2021). Analysis of lower GWP and flammable alternative refrigerants. *International Journal of Refrigeration*, 126, 12-22.
https://doi.org/10.1016/j.ijrefrig.2021.01.022

Yilmaz A. C. (2020). Performance evaluation of a refrigeration system using nanolubricant. *Applied Nanoscience*, 10(5), 1667-1678.
https://doi.org/10.1007/s13204-020-01258-5

Zawawi N. N. M., Azmi W. H., Redhwan A. A. M., Ramadhan A. I., & Ali H. M. (2022). Optimization of air conditioning performance with Al_2O_3-SiO_2/PAG composite nanolubricants using the response surface method. *Lubricants*, 10, 243.
https://doi.org/10.3390/lubricants10100243